JAAS Journal of Analytical Atomic Spectrometry Zircon water content: reference material development and simultaneous measurement of oxygen isotopes by SIMS †

Article · June 2019

DOI: 10.1039/c9ja00073a

CITATIONS
2

READS
99

7 authors, including:

Xiaoping Xia
Chinese Academy of Sciences
147 PUBLICATIONS **6,377** CITATIONS
SEE PROFILE

Wancai Li
University of Science and Technology of China
10 PUBLICATIONS **116** CITATIONS
SEE PROFILE

Wanfeng Zhang
Chinese Academy of Sciences
25 PUBLICATIONS **92** CITATIONS
SEE PROFILE

Qing Yang
Chinese Academy of Sciences
16 PUBLICATIONS **35** CITATIONS
SEE PROFILE

Volume 34 | Number 6 | June 2019 | Pages 1037–1296

JAAS

Journal of Analytical Atomic Spectrometry

rsc.li/jaas

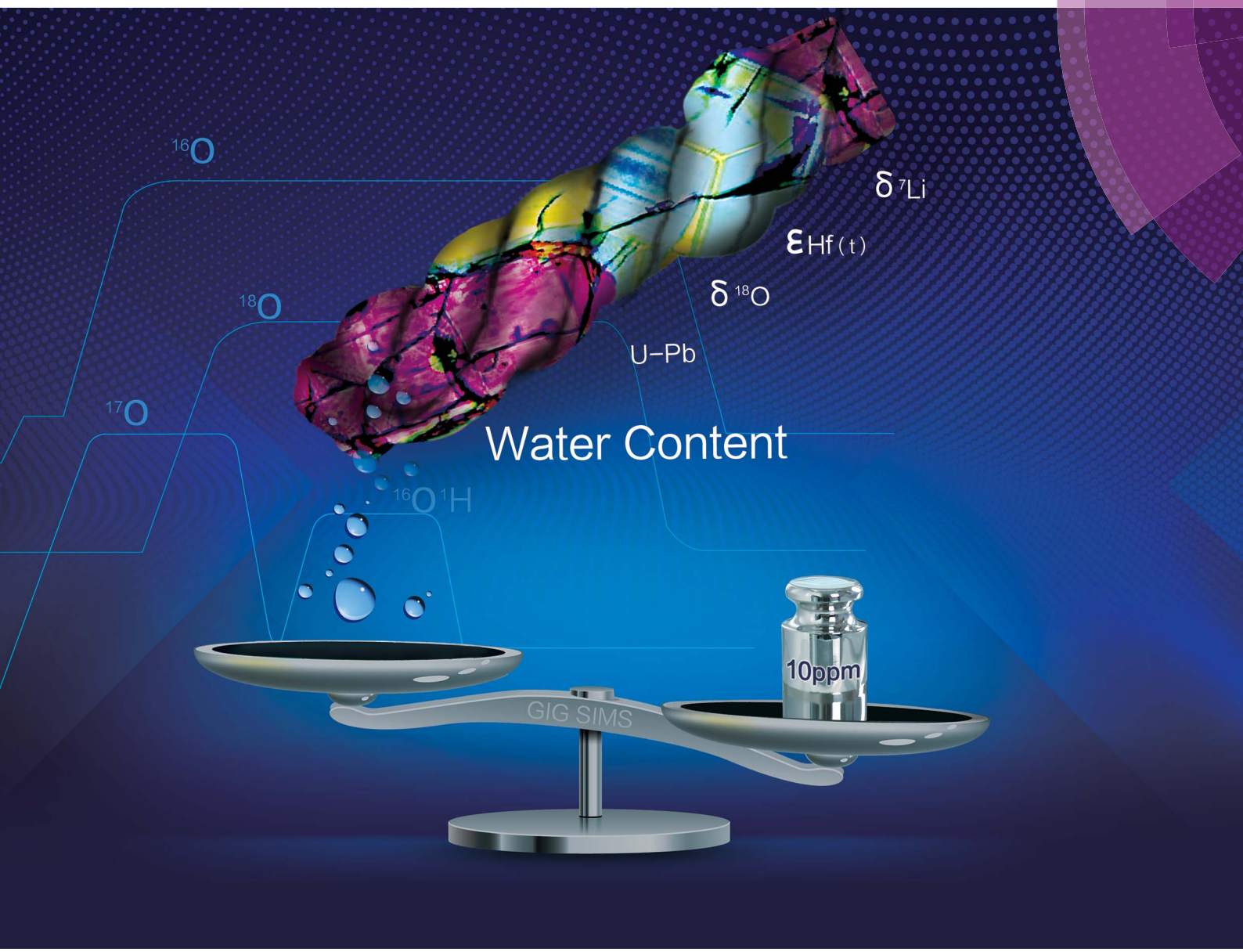

ISSN 0267-9477

ROYAL SOCIETY OF CHEMISTRY | Celebrating IYPT 2019

PAPER

Xiao-Ping Xia *et al.*

Zircon water content: reference material development and simultaneous measurement of oxygen isotopes by SIMS

JAAS

PAPER

Cite this: *J. Anal. At. Spectrom.*, 2019, **34**, 1088

Zircon water content: reference material development and simultaneous measurement of oxygen isotopes by SIMS†

Xiao-Ping Xia, *[a] Ze-Xian Cui,[ab] Wancai Li,[c] Wan-Feng Zhang,[a] Qing Yang,[a] Hejiu Hui[d] and Chun-Kit Lai[ef]

Zircon water content is an important physicochemical parameter for many geological processes, yet its measurement by the secondary ion mass spectrometry (SIMS) technique is hampered by the lack of suitable reference materials and high water background, especially if large-geometry (LG)-SIMS is used. Here we have described a suite of newly developed reference materials for SIMS zircon water content analysis and a modified micro-analytical technique (using a CAMECA IMS 1280-HR SIMS) that can simultaneously measure the zircon water content and oxygen isotopes. A total of 20 natural zircon grains/sherds were analyzed *via* Fourier transform infrared spectroscopy (FTIR), among which 8 (with good water content result reproducibility) were further analyzed by SIMS. Before the SIMS analysis, FTIR analyzed sample blocks were mounted with a Sn-based alloy to minimize degassing and background water. As in routine SIMS oxygen isotope measurement, $^{16}O^-$ and $^{18}O^-$ were collected using two Faraday cups, and in addition $^{16}O^1H^-$ was simultaneously measured using an electron multiplier. The measured $^{16}O^1H/^6O$ ratio was converted into water content, using a calibration line established based on SIMS $^{16}O^1H^-/^{16}O^-$ ratios *vs.* the FTIR water content. Both the internal and external precisions of corrected $\delta^{18}O$ are <0.4 permil (2SE or 2SD). The internal precision of $^{16}O^1H^-/^{16}O^-$ ratios follows a Poisson error theoretical trend and is generally better than 0.3%. The external precision (reproducibility) of $^{16}O^1H^-/^{16}O^-$ ratios is better than 5% (2SD) for homogenous samples, and uncertainty of the calibrated water content is ~10%.

Received 25th February 2019
Accepted 29th March 2019

DOI: 10.1039/c9ja00073a

rsc.li/jaas

1. Introduction

Zircon is a common accessory mineral in a wide range of rock types. It is widely regarded to be the best geochronometer due to its relatively high U and low common Pb content.[1] Significant achievements have been made in zircon U–Pb dating in terms of advancement of the technique and widening its applications.[2,3] Zircon contains a high Hf content and has a low Lu/Hf ratio and is also ideal for Hf isotope studies.[4,5] With the development of secondary ion mass spectrometry (SIMS), high precision analysis of zircon O–Li isotopes and trace element compositions can be achieved.[6,7] The water content in nominally anhydrous minerals (NAMs) has a major influence on mineral and rock properties such as mechanical strength and electrical conductivity.[8,9] Previous studies have shown that water (up to 10^3 ppm) can be incorporated into non-metamict zircons,[10] which has potential for use in evaluating water in melts. However, the determination of the water content in zircon is highly challenging due to the lack of suitable analytical methods. Cathodoluminescence (CL)-imaging and *in situ* micro-analyses of U–Pb geochronology by laser ablation inductively coupled plasma mass spectrometry (LA-ICPMS) or SIMS clearly demonstrated the existence of multiple growth domains within a single zircon grain, and therefore high spatial resolution analytical techniques are required for zircon water content measurements.[3] Fourier transform infrared spectroscopy (FTIR) is most commonly used to determine the water content in glasses and minerals, yet this technique requires a sample size of over 80 × 80 μm,[11] which is larger than many natural zircon grains. Other disadvantages of FTIR include that its results are strongly dependent on crystallographic orientation, and that it cannot be used to measure oxygen isotopes. SIMS analysis is routinely

[a]*State Key Laboratory of Isotope Geochemistry, Guangzhou Institute of Geochemistry, Chinese Academy of Sciences, Guangzhou 510640, China. E-mail: xpxia@gig.ac.cn*
[b]*University of Chinese Academy of Sciences, Beijing 100049, China*
[c]*School of Earth and Space Science, The University of Science and Technology of China, Hefei 230026, China*
[d]*State Key Laboratory for Mineral Deposits Research & Lunar and Planetary Science Institute, School of Earth Sciences and Engineering, Nanjing University, Nanjing 210046, China*
[e]*Faculty of Science, Universiti Brunei Darussalam, Gadong BE1410, Brunei Darussalam*
[f]*Centre of Excellence in Ore Deposits (CODES), University of Tasmania, Tasmania 7001, Australia*

† Electronic supplementary information (ESI) available. See DOI: 10.1039/c9ja00073a

used to measure water concentrations in geological samples, yet the most commonly used instrument (CAMECA IMS 3f-7f) cannot yield high-precision isotope data either, which is important to trace the origin of water or zircon itself. Although we can obtain isotope ratios in another independent analytical run, it is difficult to ensure the coupling of the two datasets as zircon is commonly heterogeneous (*e.g.*, inherited core and overgrown rim). Recent studies have shown that large-geometry (LG)-SIMS has the potential to simultaneously determine the water content and oxygen isotopes,[11] with the sole technical barrier being the relatively high vacuum pressures and thus high water background.

In this work, we have developed a new suite of zircon water content reference materials and introduced a modified analytical procedure to simultaneously determine the zircon water content and oxygen isotopes using a CAMECA IMS 1280-HR, which limited the analytical water background to <10 ppm. The major technical advancements employed include a (1) tin-based alloy for sample preparation to reduce degassing and (2) liquid nitrogen to cool the analysis chamber and improve the vacuum. This simultaneous measurement technique for zircon water content and oxygen isotope compositions not only doubles the efficiency of LG-SIMS (which generally has a heavy loading), but also avoids the decoupling of water content and oxygen isotope analysis results.

2. Samples and sample preparation

In order to find zircons suitable for water content reference, a total of 20 natural zircon grains/sherds were investigated. All of them are large megacrystic zircons and were chosen either due to their gem quality (*i.e.*, with minimal inclusions or structural defects) or because they are conventional standards for U–Pb or Hf–O isotope micro-analyses, such as 91500,[12] GJ-1,[13] , Plesovice,[14] CN92-1 (ref. 15) and Penglai.[16] All the samples were purchased from jewelry suppliers or collected from different localities including Eastern China, southern Thailand and Northern Territory (NT) and New South Wales (NSW) of Australia. They were first checked under a microscope for obvious impurities and then analyzed using FTIR to check the homogeneity of water contents. Consequently, only eight cut sherds from these samples, including two widely used U–Pb age and Hf–O isotope reference samples (91500 and GJ-1), were qualified for further SIMS analyses. These samples are described briefly here. The zircon 91500 sherd analyzed here was obtained from IAgeo. It is pink, transparent and has a size of 0.5 × 1.5 mm. The GJ-1 sherd (size of 1 × 3 mm) was obtained from GEMOC (ARC National Key Centre for Geochemical Evolution and Metallogeny of Continents, Macquarie University, Australia). Zircon ZG3 and ZG7 are gem-quality cut stones, purchased from jewelry suppliers. They were obtained from Sri Lanka, yet no other geological information is available. Zircon ZG3 (~18 mm long and weight ~4.5 g) is dark brown and transparent. It contains very few impurities when observed under a binocular microscope, and a fragment (1 × 2 mm) of this gemstone was used in this study. Zircon ZG7 (~20 mm long and weight ~5 g) is red and translucent. The tiny inclusions (size: ~10 μm) found under the microscope were avoided in the later SIMS and FTIR analyses. Zircon ZG6 (size: 3 × 2 mm) fragments were derived from a large (size: 52 × 45 × 42 mm and weight ~70 g) zircon block from Mudtank (NT, Australia). Both zircon D15395-3 and D15395-4 were collected from Rocky River (Uralla, NSW, Australia), and zircon D16314 was from Bald Nob Creek (Glen Innes, NSW, Australia). All these three zircons are alluvial grains (size: ~1 cm) liberated from megacrysts in local high Al-basalts, and sherds (size: 2 × 2 mm) from each of these samples were analyzed in this study.

After the FTIR analysis, all the samples were placed on a double adhesive tape and enclosed in a Sn-based alloy (52% Sn + 48% Cr) according to the method described by Zhang *et al.*[17] The alloy has a melting point of ~90 °C and a Brinell hardness of 20. It was used to replace epoxy resins, which continuously degas hydrocarbons and water under vacuum and increase the water background. The Sn-based alloy mount was photographed under reflected light microscopy and then coated with a ~30 nm thick gold film before the SIMS analysis.

3. Experiments

3.1 FTIR

The analysis was conducted at the School of Earth and Space Science, University of Science and Technology of China (USTC). A PerkinElmer Frontier spectrometer coupled with a Spotlight 200 microscope was used. Zircon samples were cut according to their original shape using a diamond fret saw and polished to cuboid blocks with three mutually perpendicular planes in random directions. Optically clean and inclusion/crack-free zircon cuboid blocks were chosen for the analyses. The actual thickness of the zircon blocks was measured using a Mitutoyo digital micrometer, with an error of 1–2 μm yielded by multiple measurements (Table 1). FTIR spectra were obtained using a polarized transmission model from three mutually perpendicular planes of the zircon blocks (Fig. 1). A total of 256 scans were accumulated for each spectrum in the 4000 to 1000 cm^{-1} range with a globar source, a KBr beam splitter, a ZnSe wire grid polarizer, and a liquid nitrogen-cooled mercury cadmium telluride (MCT) detector with 100 × 100 μm aperture and 4 cm^{-1} resolution. The sample stage is housed in a Perspex chamber, which is continuously flushed with purified nitrogen gas to suppress the atmospheric water background. For each sample, 5 to 7 analyses were conducted in each direction plane in different positions to check the spatial homogeneity of the water content. The spectra with similar shapes and an integrated areal variation within 10% (1SD) were considered as homogeneous, and their average value was used to calculate the total water content. The spectral baseline corrections were implemented by performing a spline fit defined by points outside the integrated region. The integrated area was calculated after baseline correction and normalized to 1 cm thickness, in the 3600 to 3000 cm^{-1} range. Water contents were calculated based on the modified version of the Beer–Lambert law:

Table 1 Analytical results of FTIR

Sample	Thickness[a]	Thickness[b]	A_x[c] (cm^{-2})	A_y (cm^{-2})	A_z (cm^{-2})	A_i (cm^{-2})	H_2O	SD (%)
ZG7	1.093	1.143	247.9	275.9	252.46	776.26	83.0	2.3
ZG6	0.858	1.425	109.7	242.93	288.46	641.09	68.5	5.7
D16314-2	1.465	1.379	94.79	87.41	62.63	244.83	26.2	1.7
91500	0.570	0.776	142.43	175.38	214.28	532.09	56.9	3.5
GJ-1	0.780	0.771	309.48	322.99	358.93	991.4	106.0	5.7
ZG3	1.294	0.776	135.41	108.76	142.68	386.85	41.4	1.5
D15395-3	0.850	0.705	1371.11	1651.73	1702.68	4725.52	505.2	3.7
D15395-4	0.881	0.871	2502.63	2475.42	2610.56	7588.61	811.2	8.2

[a] Thickness of zircon in directions x and y. The unit is mm. [b] Thickness of zircon in direction z. The unit is mm. [c] A is the integrated area, which has been normalized to 1 cm thickness.

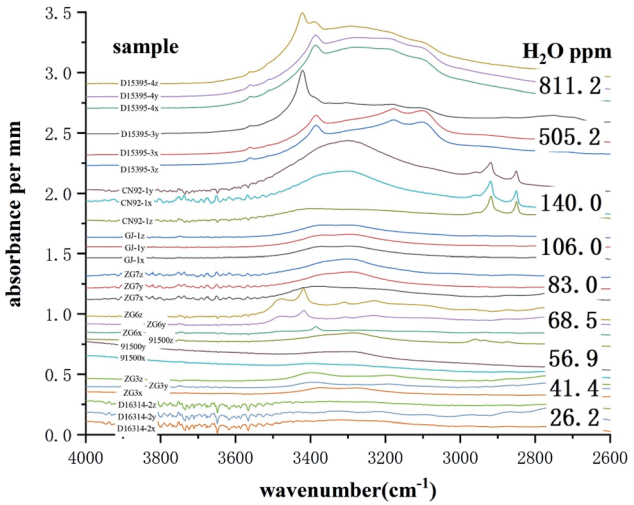

Fig. 1 FTIR spectra of the zircon samples.

$$C = A/(\varepsilon \times t)$$

where C is the water content, A is the integrated area, ε is the calibration absorption coefficient and t is the sample thickness. The total integrated area (A) is equal to the sum of integrated areas in the three mutually perpendicular directions, *i.e.*, $A = A_{x'} + A_{y'} + A_{z'}$.[18] Using the absorption coefficient ε of 36 241 cm^{-2} per mol H_2O/L (Trail *et al.*[19]), the calculated water contents are listed in Table 1.

3.2 SIMS

SIMS analysis was carried out with a CAMECA IMS 1280-HR at the SIMS laboratory of Guangzhou Institute of Geochemistry, Chinese Academy of Sciences (GIGCAS). The IMS 1280-HR inherits certain important features for high-precision stable isotope measurements from its pioneering IMS 1280 model. These features include automatic centering of the secondary beam to correct for tiny sample geometric variations and nuclear magnetic resonance (NMR) magnet control with long-term stability. Compared with IMS 1280, IMS 1280-HR has a higher mass resolution capability and higher turbo pumping speed (500 l s^{-1} *vs.* 300 l s^{-1}) in the analysis chamber, together with bakeout facility of the flight tube inside the magnet. These improvements give the IMS 1280-HR an ultimate vacuum of 3×10^{-10} mbar in the analysis chamber with the source off and without the sample after a baking up operation of 24 hours and two weeks of pumping, which enhances its water content measurement capability.

By cooling a ring located in the sample chamber to liquid nitrogen temperature (−196 °C), it is possible to improve the vacuum condition in the analysis chamber. Before loading into the analysis chamber, the alloy sample mount was placed in a storage chamber overnight and further pumped down (for 1 to 2 hours) in the analysis chamber to 2.7×10^{-9} mbar before the analysis.

A Cs^+ primary beam (3–5 nA) with an impact energy of 10 kV was used to sputter secondary ions from zircon samples. The size of the analytical area was about 30 × 30 μm (15 μm spot size + 15 μm rastering). A normal-incidence electron gun was used to ensure charge compensation, and a nuclear magnetic resonance (NMR) controller was used to stabilize the magnetic field. Other analytical conditions include a 400 μm contrast aperture, ~60 μm entrance slit, and 50 eV energy slit with a 5 eV energy window. To minimize water background signals, a narrow field aperture was used. ^{16}O and ^{18}O ions are detected using two Faraday cup detectors with resistors of 10^{10} Ohm and 10^{11} Ohm respectively, while $^{16}O^1H$ is simultaneously measured using an electron multiplier. For ^{16}O and ^{18}O, 500 μm collector slits were used to yield a ~2500 MRP, while ~173 μm collector slits (corresponding to a ~7000 MRP) were used for $^{16}O^1H$ to avoid ^{17}O interference. Under such conditions, ~4×10^8 counts per s per nA were detected for ^{16}O. A single spot analysis lasts for ~4.5 minutes, including 200 seconds pre-sputtering and automatic centering in the secondary optics (centering DTFA and DTCA) and ~1 min to integrate 16 cycles of static analysis of $^{16}O^1H/^{16}O$ and $^{18}O/^{16}O$. The pre-sputtering process was conducted to raster an area of 50 × 50 μm, which is larger than the analysis area to minimize the water background signal.

4. Results

4.1 FTIR

The results and calibrated water content for all the zircon samples are listed in Table 1, and the spectra are shown in Fig. 1. All the spectra are similar irrespective of the total

absorbance. The narrow absorption bands confirm that all the zircon samples have received a low radiation dosage and are therefore not metamict, as metamict zircons commonly have broad (3600 to 2900 cm^{-1}) and non-polarized absorption bands.[20] Sample D16314-2 yielded the lowest value (244.83 cm^{-2}) of the total integrated area of the FTIR spectra while D15395-4 yielded the highest one (7588.61 cm^{-2}). The calibrated water contents of all the samples range from 26 to 811 ppm. The standard deviation of the multiple analyses varies from 1.5 to 8.2% for these selected samples (Table 1). It should be noted that the samples with higher standard deviation (>10%) than these eight samples were not considered here. The uncertainty in the thickness of the sample is only about 0.1%, which is much lower than that of the area integration and is thus negligible.

4.2 SIMS

Detailed $^{16}O^{1}H/^{16}O$ and $^{18}O/^{16}O$ ratios obtained are listed in Table 2 (summarized in Table 3). The average of measured $^{16}O^{1}H/^{16}O$ ratios (plotted in Fig. 2) for the samples ranges from 2.93×10^{-6} (sample 16314-2) to 1.65×10^{-4} (sample 15395-4) (Table 3). Internal precision of a single spot analysis (for $^{16}O^{1}H/^{16}O$) is determined by the reproducibility of data cycles for one analytical spot (standard error of the mean), which ranges generally from <0.1% (D15395-4; 2SE) to ~0.3% (D16314-2; 2SE) (Table 2). Some exceptionally low-precision analyses (up to 1.64%, *e.g.*, spot ZG7@2) are also presented (for more discussion refer to Section 5.1). The spot-to-spot external precision (reproducibility) for $^{16}O^{1}H/^{16}O$ ratios ranges from 1.32% (ZG3 and 2SD) to 20.38% (ZG6 and 2SD) (Table 3). The gem-quality sample ZG3 yielded the best precision, and some samples (*e.g.*, D15395-4, GJ-1 and D16314-2) show a spot-to-spot external precision better than 5% (2SD). Samples 91500 and ZG7 are of gem-quality but with modest external reproducibility (~10%, 2SD) due to some isolated data points with low internal precision (Fig. 2). The D15395-3 and ZG6 zircons yielded a remarkably higher value (16.20 and 20.38%) than other samples (Table 3).

All the measured oxygen isotope data were normalized to measurement of the 91500 zircon (with a recommended $\delta^{18}O$ value of 9.94 ± 0.10, 2SD)[21] and reported with reference to SMOW. The internal precision of a single spot analysis reported here (Table 2) is the analytical internal error added in quadrature by repeatability of the standard sample (91500, 2SD = 0.3‰; this study). The average normalized $\delta^{18}O$ values for all the samples analyzed are from 4.79 ± 0.36 (ZG6, 2SD) to 12.45 ± 0.39 (ZG3; 2SD) (Table 3). The measured value of 4.79 ± 0.34 (2SD) for ZG6 is similar to the recommended value (5.03 ± 0.20, 2SD) for the UW-MT[6] zircon collected from the same location. The three samples (D16314-2, D15395-4, and D15395-3) yielded mantle oxygen isotope compositions, consistent with its interpreted mantle origin.[22] It is noteworthy that a relatively high $\delta^{18}O$ value (12.45 ± 0.39, 2SD) was obtained for the ZG3 zircon from Sri Lanka, a country in which the presence of high $\delta^{18}O$ zircons was well documented.[23] The internal precisions (single spot $\delta^{18}O$; both analytical error and uncertainty of external standardization were included) of the analyses are generally <0.4‰ (2SE, Table 2), which is very similar to the spot-to-spot external precisions for $\delta^{18}O$ (<0.4‰, 2SD) (Table 3).

5. Discussion

5.1 Analytical precision

The analytical precision discussed here indicates the precision of within-spot analysis (internal precision, 2SE) and external precision (reproducibility) of spot-to-spot analysis (2SD). The uncertainty of external calibration of the water content will be discussed in Section 5.3. Considering that the ^{16}O signal intensity is much higher than that of $^{16}O^{1}H$, the $^{16}O^{1}H/^{16}O$ ratio uncertainties can be expected from the counting statistics of the $^{16}O^{1}H$ signal intensity (Poisson error). The plot of internal precision of our data *vs.* $^{16}O^{1}H$ signal intensity (Fig. 3) shows that measured analytical errors decrease quickly with increasing $^{16}O^{1}H$ signal intensities between 5000 and 15 000 cps and reach about 0.2% with the $^{16}O^{1}H$ signal intensity > 15000 cps. Most of the analytical error follows a Poisson error theoretical trend while some much bigger errors occurred. We interpret that it likely resulted from heterogeneity of the analyzed profile. As these analytical results are also prone to yield a higher $^{16}O^{1}H/^{16}O$ ratio (Fig. 2), we think that water-rich micro-inclusions or micro-cracks have been encountered during the secondary ion sputtering. Previous U–Pb dating[26] and oxygen isotope analysis[27] studies have also shown the existence of micro-inclusions or micro-cracks, which are too small to be detected by transmission/reflection spectral imaging. We assumed these data with an analytical error beyond 3 times the Poisson error (red dots in Fig. 2) to be affected by sample heterogeneity. After removing these data, the spot-to-spot external precision for $^{16}O^{1}H/^{16}O$ ratios of samples 91500, ZG6 and ZG7 is much improved (Table 3). However, samples ZG6 and D15395-3 still show a much higher analytical error than the other samples. We note that some data points are outliers (beyond the 3SD error), although they have internal precision similar to the expected values. In this study, we also assume that these data were obtained from heterogeneities within the samples, although more studies are required to confirm this. With the removal of these isolated data points, all the samples have a spot-to-spot external precision better 8%, and both ZG3 and ZG7 have a precision better that 2% (Table 3).

5.2 Background

It is well accepted that the water ($^{16}O^{1}H$) background measured by SIMS is related to residual H_2O in the vacuum, which is adsorbed onto or desorbed from the sample surface. Previous studies have clearly shown that the measured background hydrogen counting rates (H_{cps})[24] or $^{16}O^{1}H/^{16}O$ ratios[25] are closely correlated to the vacuum condition of the analysis. As suggested by Turner *et al.*,[11] most published SIMS water content analyses on melt inclusions and NAMs were conducted using small-geometry SIMS such as the CAMECA f-series. A low vacuum pressure (in the order of 8×10^{-10} mbar) was

Table 2 SIMS results of $^{16}O^{1}H/^{16}O$ and $^{18}O/^{16}O$ ratios

Sample no.	PI[a]	^{16}O cps	$^{16}O^{1}H/^{16}O$	2SE[b]	$^{18}O/^{16}O$	2SE[b]	$\delta^{18}O_c$	2SE[c]
Sample ZG7								
1	4.9	2.1×10^9	1.83×10^{-5}	0.12	0.0020195	0.013	6.30	0.33
2	4.8	2.1×10^9	2.03×10^{-5}	1.64	0.0020189	0.027	6.01	0.40
3	4.9	2.1×10^9	2.02×10^{-5}	0.29	0.0020189	0.018	6.01	0.35
4	4.8	2.1×10^9	1.83×10^{-5}	0.12	0.0020188	0.013	5.97	0.33
5	4.8	2.1×10^9	1.87×10^{-5}	0.14	0.0020184	0.018	5.77	0.35
6	4.8	2.1×10^9	2.23×10^{-5}	1.23	0.0020189	0.015	5.99	0.33
7	4.8	2.1×10^9	1.83×10^{-5}	0.15	0.0020190	0.016	6.08	0.34
8	4.8	2.1×10^9	2.06×10^{-5}	1.02	0.0020191	0.018	6.11	0.35
9	4.8	2.1×10^9	1.84×10^{-5}	0.12	0.0020193	0.017	6.21	0.35
10	4.8	2.1×10^9	1.84×10^{-5}	0.13	0.0020189	0.022	6.03	0.37
11	4.8	2.1×10^9	1.84×10^{-5}	0.15	0.0020188	0.012	5.94	0.32
12	4.7	2.1×10^9	1.85×10^{-5}	0.14	0.0020186	0.013	5.87	0.33
13	4.7	2.0×10^9	1.89×10^{-5}	0.12	0.0020188	0.023	5.95	0.38
14	4.4	2.0×10^9	1.85×10^{-5}	0.15	0.0020192	0.018	6.17	0.35
15	4.4	2.0×10^9	1.84×10^{-5}	0.12	0.0020192	0.019	6.16	0.36
Sample ZG6								
1	4.9	2.1×10^9	1.11×10^{-5}	1.17	0.0020164	0.015	4.76	0.34
2	4.9	2.1×10^9	1.47×10^{-5}	0.52	0.0020158	0.012	4.46	0.32
3	4.9	2.1×10^9	1.26×10^{-5}	0.49	0.0020161	0.015	4.61	0.33
4	4.9	2.1×10^9	1.43×10^{-5}	0.62	0.0020167	0.018	4.93	0.35
5	4.9	2.1×10^9	1.19×10^{-5}	1.57	0.0020162	0.018	4.69	0.35
6	4.9	2.1×10^9	1.08×10^{-5}	0.23	0.0020158	0.017	4.47	0.35
7	4.8	2.1×10^9	1.13×10^{-5}	0.27	0.0020164	0.014	4.77	0.33
8	4.1	1.8×10^9	1.31×10^{-5}	0.15	0.0020163	0.017	4.72	0.35
9	4.0	1.8×10^9	1.13×10^{-5}	0.16	0.0020165	0.021	4.80	0.36
10	4.0	1.8×10^9	1.15×10^{-5}	0.19	0.0020170	0.027	5.07	0.40
11	4.1	1.8×10^9	1.14×10^{-5}	0.16	0.0020166	0.019	4.87	0.35
12	4.0	1.8×10^9	1.09×10^{-5}	0.19	0.0020160	0.016	4.58	0.34
13	4.0	1.8×10^9	1.11×10^{-5}	0.18	0.0020165	0.025	4.80	0.39
14	4.0	1.8×10^9	1.16×10^{-5}	0.23	0.0020165	0.018	4.81	0.35
15	4.1	1.8×10^9	1.12×10^{-5}	0.16	0.0020167	0.017	4.94	0.34
Sample D16314-2								
1	4.4	1.9×10^9	2.89×10^{-6}	0.31	0.0020173	0.014	5.22	0.33
2	4.3	1.9×10^9	2.95×10^{-6}	0.30	0.0020177	0.019	5.40	0.36
3	4.3	1.9×10^9	2.89×10^{-6}	0.31	0.0020180	0.019	5.54	0.36
4	4.4	2.0×10^9	2.95×10^{-6}	0.35	0.0020175	0.017	5.31	0.34
5	4.4	2.0×10^9	2.99×10^{-6}	0.30	0.0020178	0.022	5.45	0.37
6	4.4	2.0×10^9	2.94×10^{-6}	1.32	0.0020177	0.023	5.39	0.38
7	4.3	1.9×10^9	3.00×10^{-6}	0.30	0.0020171	0.016	5.14	0.34
8	4.3	1.9×10^9	2.95×10^{-6}	0.34	0.0020173	0.020	5.21	0.36
9	4.3	1.9×10^9	2.83×10^{-6}	0.39	0.0020174	0.016	5.25	0.34
10	4.3	1.9×10^9	2.93×10^{-6}	0.30	0.0020169	0.020	5.01	0.36
11	4.3	1.9×10^9	2.84×10^{-6}	0.31	0.0020177	0.014	5.40	0.33
12	4.3	1.9×10^9	3.03×10^{-6}	0.38	0.0020177	0.016	5.43	0.34
13	4.4	1.9×10^9	2.87×10^{-6}	0.32	0.0020177	0.021	5.40	0.37
14	4.3	1.9×10^9	3.04×10^{-6}	0.30	0.0020172	0.015	5.15	0.34
15	4.2	1.9×10^9	2.89×10^{-6}	0.35	0.0020178	0.019	5.49	0.35
Sample 91500								
1	3.9	1.8×10^9	1.42×10^{-5}	0.15	0.0020271	0.021	10.09	0.37
2	3.9	1.8×10^9	1.40×10^{-5}	0.15	0.0020268	0.018	9.93	0.35
3	3.9	1.7×10^9	1.36×10^{-5}	0.44	0.0020270	0.020	10.05	0.36
4	3.9	1.7×10^9	1.45×10^{-5}	0.17	0.0020269	0.032	9.99	0.44
5	3.9	1.7×10^9	1.33×10^{-5}	0.15	0.0020274	0.019	10.26	0.35
6	3.9	1.7×10^9	1.32×10^{-5}	0.16	0.0020271	0.022	10.09	0.37
7	3.9	1.8×10^9	1.40×10^{-5}	0.15	0.0020265	0.016	9.82	0.34
8	3.9	1.8×10^9	1.49×10^{-5}	0.19	0.0020267	0.024	9.91	0.38
9	3.9	1.7×10^9	1.62×10^{-5}	1.86	0.0020264	0.019	9.76	0.36
10	3.9	1.7×10^9	1.35×10^{-5}	0.21	0.0020262	0.020	9.65	0.36
11	3.8	1.7×10^9	1.35×10^{-5}	0.22	0.0020268	0.015	9.93	0.34

Table 2 (*Contd.*)

Sample no.	PI[a]	^{16}O cps	$^{16}O^{1}H/^{16}O$	2SE[b]	$^{18}O/^{16}O$	2SE[b]	$\delta^{18}O_c$	2SE[c]
12	3.8	1.8×10^9	1.32×10^{-5}	0.19	0.0020267	0.018	9.89	0.35
13	3.8	1.7×10^9	1.35×10^{-5}	0.17	0.0020269	0.014	9.98	0.33
14	3.9	1.7×10^9	1.32×10^{-5}	0.15	0.0020265	0.026	9.79	0.40
15	3.9	1.7×10^9	1.33×10^{-5}	0.21	0.0020267	0.030	9.90	0.43
Sample GJ-1								
1	3.8	1.8×10^9	1.93×10^{-5}	1.73	0.0020193	0.023	6.24	0.38
2	3.8	1.7×10^9	1.89×10^{-5}	0.13	0.0020196	0.021	6.36	0.37
3	3.8	1.7×10^9	1.89×10^{-5}	0.16	0.0020186	0.021	5.84	0.37
4	3.8	1.7×10^9	1.89×10^{-5}	0.13	0.0020185	0.021	5.80	0.37
5	3.8	1.7×10^9	1.91×10^{-5}	0.13	0.0020190	0.021	6.05	0.37
6	3.8	1.7×10^9	1.90×10^{-5}	0.13	0.0020192	0.020	6.16	0.36
7	3.8	1.7×10^9	1.91×10^{-5}	0.14	0.0020195	0.018	6.31	0.35
8	3.8	1.8×10^9	1.88×10^{-5}	0.13	0.0020198	0.014	6.44	0.33
9	3.8	1.8×10^9	1.87×10^{-5}	0.13	0.0020192	0.014	6.15	0.33
10	3.8	1.8×10^9	1.89×10^{-5}	0.15	0.0020190	0.026	6.08	0.40
11	3.8	1.7×10^9	1.89×10^{-5}	0.13	0.0020189	0.021	6.00	0.36
12	3.8	1.7×10^9	1.88×10^{-5}	0.13	0.0020189	0.024	6.04	0.38
13	3.8	1.7×10^9	2.00×10^{-5}	0.23	0.0020192	0.014	6.14	0.33
14	3.8	1.8×10^9	1.90×10^{-5}	0.14	0.0020195	0.020	6.31	0.36
15	3.8	1.7×10^9	1.95×10^{-5}	0.15	0.0020192	0.021	6.18	0.37
Sample ZG3								
1	3.8	1.8×10^9	9.20×10^{-6}	0.18	0.0020317	0.017	12.39	0.35
2	3.8	1.7×10^9	9.32×10^{-6}	0.18	0.0020325	0.021	12.80	0.37
3	3.8	1.7×10^9	9.13×10^{-6}	1.90	0.0020321	0.017	12.58	0.34
4	3.8	1.7×10^9	9.32×10^{-6}	0.18	0.0020320	0.019	12.53	0.36
5	3.8	1.7×10^9	9.25×10^{-6}	0.18	0.0020323	0.016	12.68	0.34
6	3.8	1.7×10^9	9.28×10^{-6}	0.18	0.0020317	0.022	12.41	0.37
7	3.8	1.7×10^9	9.32×10^{-6}	0.21	0.0020317	0.017	12.40	0.34
8	3.8	1.7×10^9	9.29×10^{-6}	0.18	0.0020320	0.018	12.53	0.35
9	3.8	1.7×10^9	9.24×10^{-6}	0.18	0.0020315	0.016	12.31	0.34
10	3.8	1.7×10^9	9.35×10^{-6}	0.18	0.0020324	0.014	12.75	0.33
11	3.9	1.7×10^9	9.30×10^{-6}	0.27	0.0020317	0.023	12.40	0.38
12	3.9	1.8×10^9	9.18×10^{-6}	0.22	0.0020317	0.012	12.40	0.32
13	3.9	1.8×10^9	9.29×10^{-6}	0.18	0.0020318	0.017	12.43	0.35
14	3.9	1.8×10^9	9.27×10^{-6}	0.21	0.0020311	0.019	12.09	0.35
15	4.0	1.7×10^9	9.33×10^{-6}	0.21	0.0020313	0.020	12.19	0.36
Sample DS5395-4								
1	3.2	1.3×10^9	1.57×10^{-4}	0.10	0.0020172	0.028	5.19	0.41
2	3.2	1.3×10^9	1.64×10^{-4}	0.06	0.0020168	0.020	4.96	0.36
3	3.2	1.3×10^9	1.71×10^{-4}	0.08	0.0020166	0.031	4.87	0.43
4	3.2	1.3×10^9	1.69×10^{-4}	0.05	0.0020173	0.027	5.25	0.41
5	3.2	1.3×10^9	1.62×10^{-4}	0.07	0.0020166	0.022	4.88	0.37
6	3.2	1.3×10^9	1.66×10^{-4}	0.05	0.0020165	0.023	4.83	0.38
7	3.2	1.3×10^9	1.65×10^{-4}	0.06	0.0020168	0.019	5.01	0.37
8	3.2	1.3×10^9	1.62×10^{-4}	0.06	0.0020169	0.032	5.04	0.36
9	3.2	1.4×10^9	1.63×10^{-4}	0.09	0.0020169	0.024	5.04	0.35
10	3.2	1.4×10^9	1.66×10^{-4}	0.07	0.0020162	0.030	4.68	0.35
11	3.2	1.4×10^9	1.68×10^{-4}	0.09	0.0020168	0.019	4.99	0.36
12	3.2	1.3×10^9	1.73×10^{-4}	0.06	0.0020172	0.017	5.17	0.35
13	3.2	1.3×10^9	1.64×10^{-4}	0.05	0.0020173	0.027	5.23	0.35
14	3.2	1.3×10^9	1.66×10^{-4}	0.06	0.0020170	0.023	5.08	0.35
15	3.2	1.3×10^9	1.65×10^{-4}	0.14	0.0020167	0.025	4.94	0.35
Sample D15395-3								
1	3.0	1.3×10^9	9.66×10^{-5}	0.18	0.0020163	0.026	4.75	0.40
2	3.0	1.2×10^9	8.93×10^{-5}	0.13	0.0020164	0.027	4.81	0.41
3	3.0	1.2×10^9	1.09×10^{-4}	0.11	0.0020171	0.024	5.12	0.38
4	3.0	1.2×10^9	1.07×10^{-4}	0.12	0.0020165	0.030	4.81	0.42
5	3.0	1.3×10^9	1.06×10^{-4}	0.12	0.0020162	0.024	4.69	0.38
6	3.0	1.2×10^9	1.08×10^{-4}	0.08	0.0020168	0.036	5.01	0.47

Table 2 (*Contd.*)

Sample no.	PI[a]	^{16}O cps	$^{16}O^1H/^{16}O$	2SE[b]	$^{18}O/^{16}O$	2SE[b]	$\delta^{18}O_c$	2SE[c]
7	3.0	1.3×10^9	1.10×10^{-4}	0.10	0.0020165	0.022	4.84	0.37
8	3.0	1.28×10^9	1.09×10^{-4}	0.15	0.0020166	0.025	4.89	0.39
9	3.0	1.22×10^9	1.24×10^{-4}	0.07	0.0020166	0.031	4.88	0.43
10	3.0	1.23×10^9	1.23×10^{-4}	0.10	0.0020169	0.026	5.06	0.40
11	3.0	1.23×10^9	1.01×10^{-4}	0.17	0.0020164	0.025	4.80	0.39
12	3.0	1.24×10^9	1.10×10^{-4}	0.10	0.0020172	0.024	5.18	0.39
13	3.0	1.23×10^9	1.08×10^{-4}	0.11	0.0020165	0.033	4.83	0.44
14	3.0	1.24×10^9	1.09×10^{-4}	0.12	0.0020165	0.016	4.82	0.34
15	3.0	1.24×10^9	1.03×10^{-4}	0.11	0.0020172	0.017	5.17	0.35

[a] Primary ion intensity in nA. [b] Analytical error of a single spot analysis determined by the reproducibility of data cycles for one analytical spot in permil. [c] Uncertainty calculated from the analytical internal error with addition of repeatability of the standard sample (0.3 permil in this study) in permil.

previously obtained with a CAMECA IMS 6f,[11] yielding a low water background (<10 ppm). The success was attributed to its small-volume source chamber, which minimized water adsorption onto the surface. In this study, we achieved a pressure of 2.7×10^{-9} mbar in the CAMECA IMS 1280-HR analysis chamber. Although this pressure is still higher than the lowest pressure reported for IMS 6f, it is remarkably lower than the lowest pressure reported for CAMECA IMS 1280 (>7.8×10^{-9} mbar).[25] The low pressure achieved in this study is largely attributed to the use of the Sn-based alloy (instead of epoxy resin) for sample preparation. Water background of the alloy mount in the vacuum (2.7×10^{-9} mbar) was estimated to be <10 ppm by repeated analyses of olivine (Fo > 90) samples, which are considered to be water-free.[17] This water background is comparable with that for IMS 6f, although the analysis pressure is higher. This is not unexpected, considering that IMS 1280-HR has much higher sensitivity at high mass resolution. We did not find any zircon samples with <10 ppm water content, and thus the water background cannot be determined directly. The lowest measured $^{16}O^1H/^{16}O$ ratio in this study is 1.91×10^{-5} (sample D16314-2), which contains 26 ppm water (FTIR results). This ratio is one order of magnitude lower than the reported ratio for zircon CZ3 (4.5×10^{-4}),[25] which is considered to contain less water and is thus used for background water estimation. Still, the ratio is one order of magnitude higher than the lowest value (2.4×10^{-6}) obtained from the water-free olivine samples analyzed under the same instrumental conditions.[17]

5.3 Water content calibration

Water contents in minerals or melt inclusions were measured by SIMS, using the relative signal intensity of ^1H or $^{16}O^1H$ (to ^{16}O, ^{18}O or ^{30}Si) with a calibration curve.[10,11,24] In this study, we measured simultaneously the zircon $^{16}O^1H/^{16}O$ ratios and their oxygen isotope compositions, which are essential for petrogenetic studies.[5,26,27] The water content calibration curves ($[H_2O] = a \times [^{16}O^1H/^{16}O] + b$) were established by comparing the FTIR results with the SIMS $^{16}O^1H/^{16}O$ ratios obtained (Fig. 4). The calibration curve is regressed using the least squares method with error weighted, which has $a = 4\ 880\ 341.5$ and $b = 5.3$. This yielded $R^2 = 0.996$, indicating very good correlation. To assess the analytical errors, all the zircon measurements were treated as unknown for calibration using the calibration curves and the results are listed in Table 4. The difference between the calibrated SIMS water contents and the FTIR results was generally < 5%, but up to 11.7% (sample 15395-4, Table 4). Therefore, the accuracy of the water content measurements was estimated here to be ~10%.

Table 3 Summary of average $^{16}O^1H/^{16}O$ and $\delta^{18}O_c$

	Average 1[a]			Average 2[b]			Average 3[c]				
Sample no.	$^{16}O^1H/^{16}O$	2SE (%)	No.	$^{16}O^1H/^{16}O$	2SE (%)	No.	$^{16}O^1H/^{16}O$	2SE (%)	$\delta^{18}O_c$[d]	2SD[d]	No.
ZG7	1.91×10^{-5}	12.51	15	1.86×10^{-5}	5.61	12	1.85×10^{-5}	1.94	6.04	0.32	11
ZG6	1.19×10^{-5}	20.38	15	1.14×10^{-5}	10.99	10	1.12×10^{-5}	4.66	4.79	0.36	9
D16314-2	2.93×10^{-6}	4.36	15	2.93×10^{-6}	4.53	14	2.93×10^{-6}	4.53	5.31	0.31	14
91 500	1.39×10^{-5}	11.92	15	1.37×10^{-5}	7.84	14	1.37×10^{-5}	7.84	9.95	0.30	14
GJ-1	1.90×10^{-5}	3.41	15	1.90×10^{-5}	3.47	14	1.89×10^{-5}	1.14	6.13	0.40	12
ZG3	9.27×10^{-6}	1.32	15	9.28×10^{-6}	1.06	14	9.28×10^{-6}	1.06	12.45	0.39	14
D15395-4	1.65×10^{-4}	4.68	15	1.65×10^{-4}	4.68	15	1.65×10^{-4}	4.68	5.01	0.32	15
D15395-3	1.08×10^{-4}	16.20	15	1.08×10^{-4}	16.20	15	1.07×10^{-4}	5.64	4.92	0.33	11

[a] No data were eliminated. [b] Data with unexpected internal error were eliminated. [c] Data beyond the 3SD error were eliminated. [d] The unit is permil.

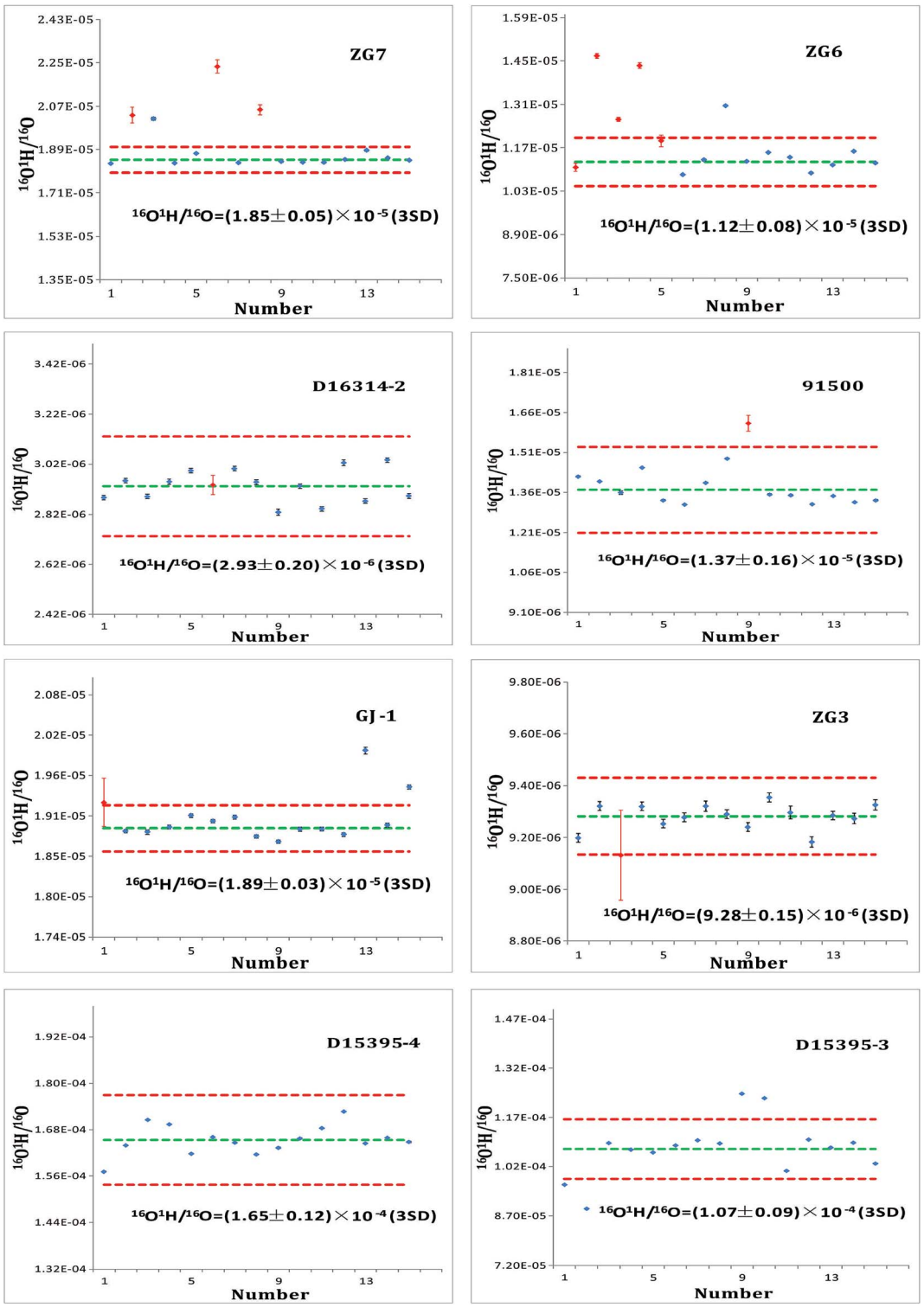

Fig. 2 SIMS analysis results of the $^{16}O^{1}H/^{16}O$ ratio.

5.4 Reference material development

A lot of zircon reference materials have been reported including, but not limited to, 91500,[12] M257,[28] Plesovice[14] and Penglai.[16] However they are generally used for U–Pb dating and Hf or O isotope studies. None of them are used as a reference material for water content calibration. In this study we first test and propose a suite of zircon reference materials for this purpose. These studied zircons generally yield < 5% (2SD) reproducibility, except for zircon 91500 that yields 7.84% (2SD) reproducibility. Considering the large variation of water content in natural zircons (<55 to 1212 ppm) even within a single sample,[10]

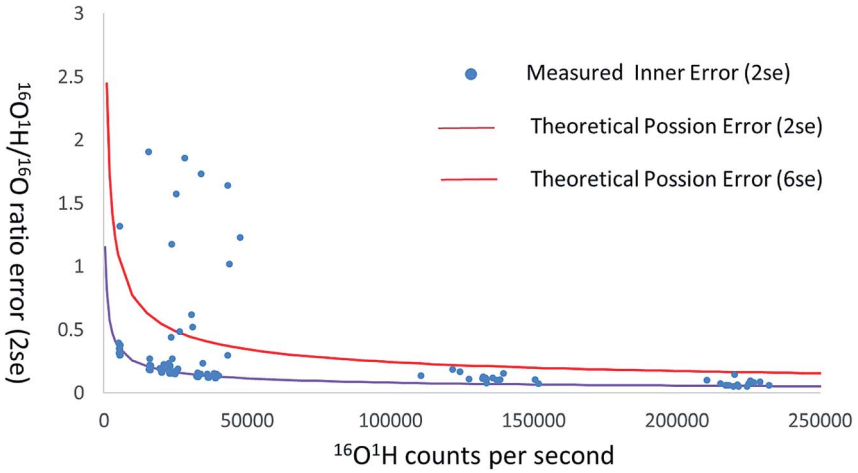

Fig. 3 Theoretical error and within-spot measured error *versus* the signal intensity.

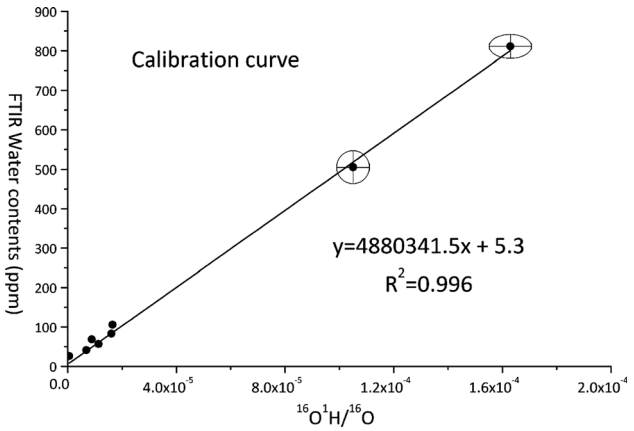

Fig. 4 Zircon water content calibration curve for SIMS analyses.

the homogeneity of these zircon samples is acceptable. Note that we have eliminated some data points from the calculation of the reproducibility. Due to substantial impurities in the zircon, six (out of 15) data points have been removed from sample ZG6, which also implies the extra care needed for using ZG6 as a reference material. It is also noteworthy that samples ZG3 and ZG7 have a very good reproducibility of <2% (2SD), and both of them have a reasonable water content (41.4 and 83.0 ppm), which can be used as a good reference material for zircon water content determination. These two zircons also have a highly homogeneous oxygen isotope composition, and can also be developed into oxygen isotope standards. Although the other zircon samples have clearly higher standard deviation than zircon ZG3, they are acceptable reference materials, especially zircon D16314-2, 91500 and D15395-4 which have essentially no impurities (none or only one analysis spot show signs of impurity). Despite the overall satisfactory performance of the zircon reference materials recommended in this study, we suggest that more zircon reference materials need to be developed, especially those with a high water content (>1000 ppm) which are not yet available at present.

Table 4 Calibrated water contents

Sample	ZG7	ZG64	D16314-2	91500	GJ-1	ZG3	D15395-4	D15395-3
H_2O (ppm)	95	60	20	72	98	51	812	530
Error[a]	3.5	−3.3	−7.2	5.9	−2.1	5.0	11.7	−10.5

[a] Error is calculated as (H_2O calibrated-H_2O FTIR)/(H_2O calibrated + H_2O FTIR) × 50%. Negative error means that calibrated SIMS results are less than those of FTIR.

6. Conclusions

Zircon water contents and oxygen isotope compositions can be simultaneously determined by using a modified technique with a CAMECA IMS 1280-HR. Sample preparation using a Sn-based alloy and liquid nitrogen cooling are effective to enhance the vacuum conditions in the analysis chamber. Both the internal precision (including uncertainty of the external standard) of individual $\delta^{18}O$ values and the spot-to-spot reproducibility are better than 0.4‰ (2SE or 2SD). The internal precision of individual $^{16}O^{1}H/^{16}O$ ratios generally follows the Poisson error theoretical trend, and the occasional larger errors likely resulted from heterogeneity of the analyzed profile. After eliminating the outlier (beyond 3SD error), the spot-to-spot reproducibility improves to ~5% (2SD). Our results suggest that these zircon samples can be used with care as zircon water content reference materials. Zircon water content calibration curves are plotted by comparing the FTIR results with the SIMS-measured $^{16}O^{1}H/^{16}O$ ratios. Accuracy of the water content measurement is estimated to be ~10% in this study.

Conflicts of interest

There are no conflicts of interest to declare.

Acknowledgements

This study was funded by the National Natural Science Foundation of China (41673010) and the Guangzhou municipal government (201607020029). Professors Min Sun and Yim Wyss from the Department of Earth Sciences, University of Hong Kong are thanked for providing the samples from New South Wales (NSW), Australia. The paper has benefited from constructive reviews by two anonymous referees. This is contribution No. IS-2677 from GIGCAS.

References

1 D. W. Davis, I. S. Williams and T. E. Krogh, in *Zircon*, ed. J. M. Hanchar and P. W. O. Hoskin, Mineralogical Soc Amer, Chantilly, 2003, vol. 53, pp. 145–181.
2 T. R. Ireland and I. S. Williams, in *Zircon*, ed. J. M. Hanchar and P. W. O. Hoskin, 2003, vol. 53, pp. 215–241.
3 J. Kosler and P. J. Sylvester, in *Zircon*, ed. J. M. Hanchar and P. W. O. Hoskin, 2003, vol. 53, pp. 243–275.
4 P. J. Patchett, O. Kouvo, C. E. Hedge and M. Tatsumoto, *Contrib. Mineral. Petrol.*, 1981, **78**, 279–297.
5 X. P. Xia, M. Sun, G. C. Zhao, F. Y. Wu, P. Xu, J. H. Zhang and Y. Luo, *Earth Planet. Sci. Lett.*, 2006, **241**, 581–593.
6 J. W. Valley, in *Zircon*, ed. J. M. Hanchar and P. W. O. Hoskin, Mineralogical Soc America, Washington, 2003, vol. 53, pp. 343–385.
7 T. Ushikubo, N. T. Kita, A. J. Cavosie, S. A. Wilde, R. L. Rudnick and J. W. Valley, *Earth Planet. Sci. Lett.*, 2008, **272**, 666–676.
8 S. D. Jacobsen, *Water in Nominally Anhydrous Minerals*, 2006, vol. 62, pp. 321–342.
9 E. Ohtani and K. D. Litasov, in *Water in Nominally Anhydrous Minerals*, ed. H. Keppler and J. R. Smyth, 2006, vol. 62, pp. 397–419.
10 J. C. M. De Hoog, C. J. Lissenberg, R. A. Brooker, R. Hinton, D. Trail, E. Hellebrand and EIMF, *Geochim. Cosmochim. Acta*, 2014, **141**, 472–486.
11 M. Turner, T. Ireland, J. Hermann, P. Holden, J. A. Padron-Navarta, E. H. Hauri and S. Turner, *J. Anal. At. Spectrom.*, 2015, **30**, 1706–1722.
12 M. Wiedenbeck, J. M. Hanchar, W. H. Peck, P. Sylvester, J. Valley, M. Whitehouse, A. Kronz, Y. Morishita, L. Nasdala, J. Fiebig, I. Franchi, J. P. Girard, R. C. Greenwood, R. Hinton, N. Kita, P. R. D. Mason, M. Norman, M. Ogasawara, P. M. Piccoli, D. Rhede, H. Satoh, B. Schulz-Dobrick, O. Skår, M. J. Spicuzza, K. Terada, A. Tindle, S. Togashi, T. Vennemann, Q. Xie and Y. F. Zheng, *Geostand. Geoanal. Res.*, 2004, **28**, 9–39.
13 M. L. A. Morel, O. Nebel, Y. J. Nebel-Jacobsen, J. S. Miller and P. Z. Vroon, *Chem. Geol.*, 2008, **255**, 231–235.
14 J. Slama, J. Kosler, D. J. Condon, J. L. Crowley, A. Gerdes, J. M. Hanchar, M. S. A. Horstwood, G. A. Morris, L. Nasdala, N. Norberg, U. Schaltegger, B. Schoene, M. N. Tubrett and M. J. Whitehouse, *Chem. Geol.*, 2008, **249**, 1–35.
15 X. Xia, M. Sun, G. Zhao, H. Li and M. Zhou, *Geochem. J.*, 2004, **38**, 191–200.
16 X.-H. Li, W.-G. Long, Q.-L. Li, Y. Liu, Y.-F. Zheng, Y.-H. Yang, K. R. Chamberlain, D.-F. Wan, C.-H. Guo, X.-C. Wang and H. Tao, *Geostand. Geoanal. Res.*, 2010, **34**, 117–134.
17 W. F. Zhang, X. P. Xia, Y. Q. Zhang, T. P. Peng and Q. Yang, *J. Anal. At. Spectrom.*, 2018, **33**, 6.
18 K. Shuai and X. Yang, *Contrib. Mineral. Petrol.*, 2017, 172.
19 D. Trail, J. B. Thomas and E. B. Watson, *Am. Mineral.*, 2011, **96**, 60–67.
20 L. Nasdala, A. Beran, E. Libowitzky and D. Wolf, *Am. J. Sci.*, 2001, **301**, 831–857.
21 M. Wiedenbeck, J. M. Hanchar, W. H. Peck, P. Sylvester, J. Valley, M. Whitehouse, A. Kronz, Y. Morishita, L. Nasdala, J. Fiebig, I. Franchi, J. P. Girard, R. C. Greenwood, R. Hinton, N. Kita, P. R. D. Mason, M. Norman, M. Ogasawara, R. Piccoli, D. Rhede, H. Satoh, B. Schulz-Dobrick, O. Skar, M. J. Spicuzza, K. Terada, A. Tindle, S. Togashi, T. Vennemann, Q. Xie and Y. F. Zheng, *Geostand. Geoanal. Res.*, 2004, **28**, 9–39.
22 A. Abduriyim, F. L. Sutherland and E. A. Belousova, *Aust. J. Earth Sci.*, 2012, **59**, 1067–1081.
23 A. J. Cavosie, J. W. Valley, N. T. Kita, M. J. Spicuzza, T. Ushikubo and S. A. Wilde, *Contrib. Mineral. Petrol.*, 2011, **162**, 961–974.
24 S. Hu, Y. T. Lin, J. C. Zhang, J. L. Hao, W. Yang and L. W. Deng, *J. Anal. At. Spectrom.*, 2015, **30**, 967–978.
25 R. T. Pidgeon, A. A. Nemchin and M. J. Whitehouse, *Geochim. Cosmochim. Acta*, 2017, **197**, 142–166.
26 P. Gao, Y. F. Zheng, Y. X. Chen, Z. F. Zhao and X. P. Xia, *Lithos*, 2018, **300**, 261–277.
27 W. Wang, P. A. Cawood, M. F. Zhou, M. K. Pandit, X. P. Xia and J. H. Zhao, *Geophys. Res. Lett.*, 2017, **44**, 10298–10305.
28 L. Nasdala, W. Hofmeister, N. Norberg, J. M. Mattinson, F. Corfu, W. Doerr, S. L. Kamo, A. K. Kennedy, A. Kronz, P. W. Reiners, D. Frei, J. Kosler, Y. Wan, J. Goetze, T. Haeger, A. Kroener and J. W. Valley, *Geostand. Geoanal. Res.*, 2008, **32**, 247–265.